

The Polarization Distribution of Eleven 3 C Radio Galaxies at 1415 MHz

G. K. Miley and H. van der Laan

Sterrewacht, Leiden

Received June 12, 1973

Summary. Total intensity and polarization distributions at 1415 MHz are given for eleven 3 C radio galaxies: 3 C 61.1; 66; 184.1; 274.1; 284; 285; 310; 314.1; 390.3; 402; and 465. The polarization structures are more complex than the total intensity distributions and for resolved components the peak polarizations

do not coincide with the brightest regions, but are generally found on steep gradients of total intensity. The morphology of the sources is discussed.

Key words: radio galaxies – polarization distributions

1. Introduction

Mapping the polarization distributions of radio galaxies and quasars requires both high resolution and good sensitivity. Usually this implies the use of an aperture synthesis instrument with a fairly complete baseline coverage. Because this is a time-consuming process for most such instruments, two-dimensional polarization distributions have so far been obtained for only a handful of sources. The Westerbork synthesis radio telescope is ideal for such studies since it is both relatively fast in operation and can determine the complete polarization state of the incoming radiation. Indeed this is one area of research for which it was originally built.

Several programmes are being carried out with the Westerbork SRT to study the brightness and polarization distributions of radio galaxies and quasars. Some results have already been published (Miley *et al.*, 1972; Miley, 1973) and others are in preparation (Fomalont and Högbom, 1973; Kronberg and Strom, 1973). In the next two years detailed studies at two or three wavelengths will encompass about fifty radio galaxies and quasars. More cursory investigations, establishing major brightness and polarization features of another two hundred such sources and the statistical properties of that sample, will also be carried out.

This paper reports observations at 1.4 GHz of eleven sources, all thought to be radio galaxies. Both total intensity and linearly polarized intensity are given. A proper interpretive discussion would be premature, since data of comparable quality are currently being acquired at 5 GHz. Many astrophysically interesting problems arise chiefly in the comparison of data sets at two or more wavelengths.

The sample selection. — The One Mile Telescope in Cambridge has mapped a large fraction of 3 C sources

in total intensity. From the maps given by Macdonald *et al.* (1968) and by Mackay (1969), we have selected eleven sources. Sources north of declination $+20^\circ$ bigger than about $6'$ were considered. After excluding sources with only two components which were unresolved or barely resolved the remaining ones identified with galaxies were inspected for strong bridges connecting the brightest components, for faint extensions from such components, and generally for complex structure resolvable with our beam. The resulting sample is a sequence of structural types from simple doubles connected by a bridge (e.g. 3 C 274.1 and 3 C 61.1) to the complexity of 3 C 66 and 3 C 465. The sample is neither complete nor unique, but does consist of sources which for our sensitivity and resolution allow measurement of many quantities of interest.

2. Observing and Reduction Procedure

The Westerbork telescope is described in detail elsewhere (Baars and Hooghoudt, 1973; Casse and Muller, 1973; Weiler, 1973) and the observing and reduction procedure used was identical to that of Miley (1973). All the sources were observed for one twelve-hour period and the measurements were calibrated using 3 C 48 and 3 C 147.

Except for 3 C 66, which was observed in August 1972, all the observations were carried out between April and September 1971. For each baseline simple linear combinations of the four output channels give the complex fringe amplitudes corresponding to the four Stokes parameters I , Q , U and V . A Fourier transform of the fringe amplitude data then gives a map of the sky

distribution of the relevant Stokes parameter over a region defined by the antenna pattern of a 25 m dish ($\sim 37'$ half-power diameter). The synthesized beam is elliptical with half-power diameters $22''$ in right ascension by $22'' \cos \delta$ in declination and the rms noise on the map is equivalent to $\sim 1.3 \times 10^{-29} \text{ Wm}^{-2} \text{ Hz}^{-1}$ ($\sim 1.3 \text{ m.f.u.}$) per synthesized beam.

All the maps included a 1.3° by 1.3° region surrounding the source. Since the diffraction grating rings of the synthesized beam were never closer than $10'$ no source was confused by its own grating rings. In a few cases however some weak intensity features were confused by grating rings from nearby background sources. The influence of these disturbing sources was removed from the entire field using a point source subtraction programme.

The maximum scale of structure that can be observed with the instrument depends on the shortest interferometer spacing used. This was either 36, 54 or 72 m. When observed with the 36 m spacing, a gaussian source of $5'$ extent would have a visibility of $\sim 80\%$. Thus smooth structures with scales much larger than $5'$ will be severely attenuated. For a 54 m and 72 m spacing the corresponding scales are $\sim 3'$ and $2.5'$.

3. The Results

Integral properties of the sources. — Table 1 lists the sources observed together with some useful additional information. A comparison of the average fringe amplitudes observed at our shortest baseline with the single-dish flux densities of Kellermann *et al.* (1969) shows what fraction of the flux is contained in the large scale structure that does not appear in our maps. Also listed are estimates of the integrated linear polarizations obtained from the average amplitudes in each of the four channels at the shortest baseline. Of course in cases like 3 C 66 and 3 C 310 where an appreciable fraction of the source flux is missing, the quoted integrated polarizations are not very meaningful. In those cases where data of other workers are available (e.g. 3 C 274.1 and 3 C 285) our results are in good agreement.

Also listed in Table 1 are the redshifts of galaxies identified with the sources, their distances estimated using a value of $75 \text{ km s}^{-1} \text{ Mpc}^{-1}$ for the Hubble Constant, their 1415 MHz luminosities, the largest angular scales observed and the corresponding linear scales. The spectral information comes from Kellermann *et al.* (1969). For 3 C 61.1 and 3 C 184.1 several objects lie within the radio contours and the exact identifications are in doubt.

Presentation of the maps. — The intensity and polarization maps are shown in Figs. 1 to 11. Following Miley (1973) we present the maps in units of flux density per synthesized beam area. For structure scales

Table 1

Source	Flux density ($10^{-26} \text{ Wm}^{-2} \text{ Hz}^{-1}$)	Shortest baseline (m)	Max. Fringe amplitude ($10^{-26} \text{ Wm}^{-2} \text{ Hz}^{-1}$)	Integrated		Largest angular size (arc seconds)	Redshift	Distance (Mpc)	1415 MHz Luminosity ($\text{WHz}^{-1} \text{ sterad}^{-1}$)	Largest linear size (kpc)	Spectrum Class α_{750}^{5000}
				polarization m (%)	ϕ (deg)						
3 C 61.1	5.8	36	5.8	6.7	43	190		780^a	(3.5×10^{25})	(718)	C ⁻ -0.95
3 C 66	9.8	36	7.3	1.5	147	415	0.0215 [1]	86	6.5×10^{23}	173	S -0.72
3 C 184.1	3.2	36	3.1	3.4	30	170	0.1187 [2]	475	6.5×10^{24}	391	C ⁻ -0.76
3 C 274.1	2.9	54	2.7	12.5	160	135		870^a	(2.2×10^{25})	(570)	C ⁻ -1.03
3 C 284	1.9	54	2.0	6.8	179	155	0.2394 [2]	957	1.6×10^{25}	719	S -0.82
3 C 285	2.2	54	2.0	6.3	44	130	0.0797 [1]	319	2.0×10^{24}	201	S -0.75
3 C 310	7.7	72	6.8	1.3	140	340	0.0543 [1]	217	3.3×10^{24}	360	C ⁻ -1.29
3 C 314.1	1.6	72	1.4	1.1	152	185		280^a [4]	(1.1×10^{24})	(250)	C ⁻ -1.09
3 C 390.3	11.6	54	9.5	6.1	5	200	0.0569 [1]	228	5.4×10^{24}	221	S -0.78
3 C 402	3.0	54	2.7	1.3	144	415	0.0247 [2]	99	2.6×10^{23}	199	C ⁻ -0.87
3 C 465	7.7	72	7.3	< 0.5	—	530	0.0301 [1]	120	9.5×10^{23}	308	C ⁻ -0.84

Ref.: [1] Burbidge and Strittmatter (1972). — [2] Burbidge *et al.* (1968). — [3] Macdonald *et al.* (1968). — [4] Mackay (1969).

^a) Distances estimated using Mackay's criterion, i.e. absolute luminosities $M_{\text{pg}} = -21.6$.

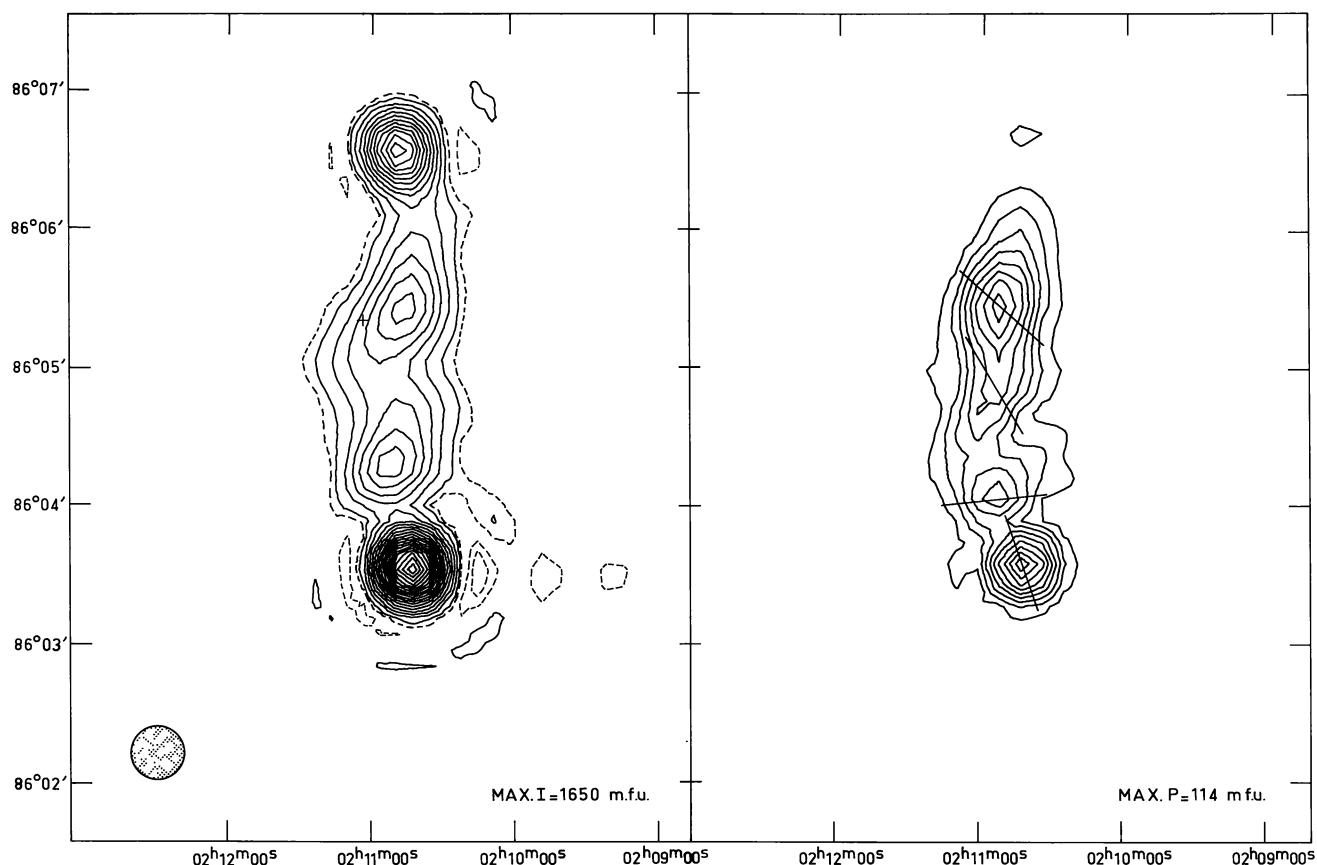


Fig. 1. 3 C 61.1. This striking source is bounded by two unresolved components of which one is 7%, the other less than 2% polarized. The bridge is resolved in width and has two broad resolved peaks elongated along the source axis. The polarization peaks in the bridge are significantly displaced from the total intensity peaks. The percentage polarization of the south edge of the inner southern component is $\sim 15\%$, while that of the inner north component reaches a level of $\sim 20\%$, as does the relative minimum in the source centre

corresponding to the range of spatial frequencies observed, conversion from the flux density S in m.f.u. to brightness temperature T in K for a source at declination δ , is given to an accuracy of $\sim 5\%$ by the formula $T = 1.21 S \sin \delta$. The polarization temperatures thus derived lie on the "BHS" scale (Berkhuijsen *et al.*, 1973); to convert to the "WSBT" scale (Westerhout *et al.*, 1962) they must be multiplied by two.

For each source we give contour maps of the total intensity, I and of the linearly polarized intensity $P = (Q^2 + U^2)^{\frac{1}{2}}$. For the total intensity maps continuous contours are plotted at 5% intervals from zero to the indicated value of MAX. I , and these are supplemented by long dashed contours representing the 2.5% level and, where appropriate, dotted contours for the -2.5% and -5% levels. For the polarization maps contours are plotted at 10% intervals from zero to the indicated value of MAX. P and the polarization position angles $\phi = \frac{1}{2} \tan^{-1}(U/Q)$ are indicated. In each figure the half-power ellipse of the synthesized beam is shown, and the optical galaxy is marked with a cross. In the cases of 3 C 61.1 and 3 C 184.1 where the identifications are doubtful the positions of the most likely optical candidate is shown.

The contour maps are uncorrected for attenuation by the $36'$ primary beam but this is always less than 6%. The angular appearance of the contours is due to the contour plotting method which interpolates linearly between the grid points on the map; these are always spaced between a half and a third of a synthesized beamwidth.

Errors in the maps. — The I , Q , U and V maps are all subject to the following additional errors: (1) random noise ~ 1.3 m.f.u. rms; (2) calibration errors $\sim 5\%$; (3) sidelobe distortion $\sim 5\%$ close to the brightest peaks; (4) distortion of the map zero level due to the missing short spacing (Miley, 1973), < 3 m.f.u. In addition, the Q , U and V maps are subject to instrumental uncertainties whose magnitude are $\sim 0.5\%$ of I . At no point on any of the V -maps was V found to be larger than 0.5% of the maximum value of I . No circular polarization is expected and its absence to this level is a partial check on the estimated errors in Q and U .

The polarized intensities $P = (Q^2 + U^2)^{\frac{1}{2}}$, position angles ($\phi = \frac{1}{2} \tan^{-1}(U/Q)$) and percentages ($m = 100P/I$) are all non-linear combinations of observable quantities and the errors, particularly for ϕ and m , are difficult to determine. However, from the above mentioned errors

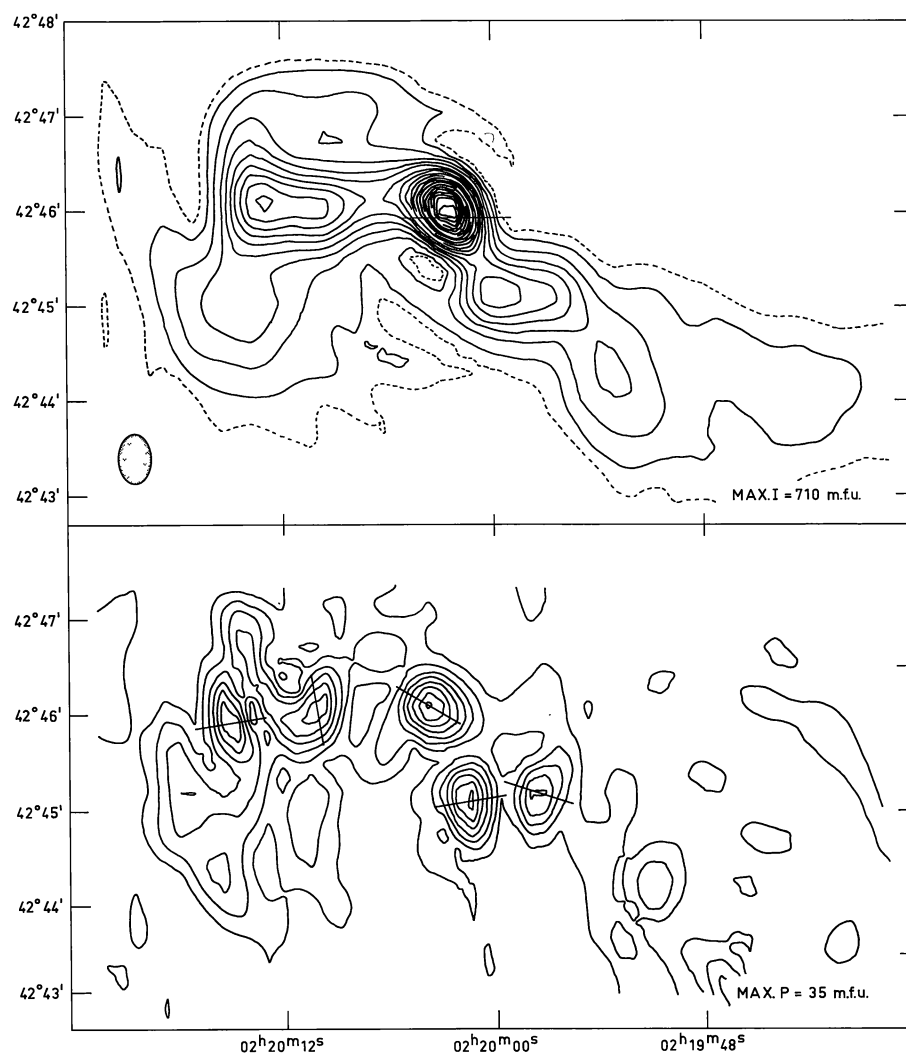


Fig. 2

Fig. 2. 3C 66. This radio galaxy, identified with an ED 2 galaxy in Abell cluster A-347 (cf. Table 1), has one of the most peculiar forms in the 3C catalogue. The main component is centred on the stellar system and has its polarization peak, $\sim 7\%$, shifted eastwards. The component to the SW of this peak has a polarization minimum at its centre and fractional polarization on its periphery reaching 17% . The same percentage polarization is obtained on the edges of the east component which also has a polarization minimum near its intensity peak

Fig. 3. 3C 184.1. This four-component source has a pronounced minimum in the centre. It consists of two bright components whose outer boundaries are unresolved and two partially resolved inner components. The NW and SE outer components are polarized by $\sim 8\%$ and 10% respectively, the inner ones by $\sim 11\%$ and 15% . The southern inner component is one of the few resolved features where the polarization and the total intensity maxima coincide. In the two NW components the polarization peaks are displaced

Fig. 4. 3C 274.1. A bridge connects the two bright components whose outer edges are unresolved. The inner gradients are partially resolved and highly polarized: both polarization peaks fall on the inner side of the total intensity maxima. Particularly the east component has a polarization peak far displaced towards the centre with a polarization percentage $\sim 15\%$. The west component has a percentage polarization in excess of 20% . The bridge polarization is less than 7% . The direction of the polarization vectors is virtually equal and the same as the direction of the integrated polarization at higher frequencies; it is nearly perpendicular to the radio axis. This implies an extremely low rotation measure (R.M. $< 5 \text{ rad. m}^{-2}$) as noted by Mitton (1972). Thus 3C 274.1 is another source whose component magnetic fields are parallel to the radio axis (Gardner and Whiteoak, 1971)

1973AJ&A...28...359M

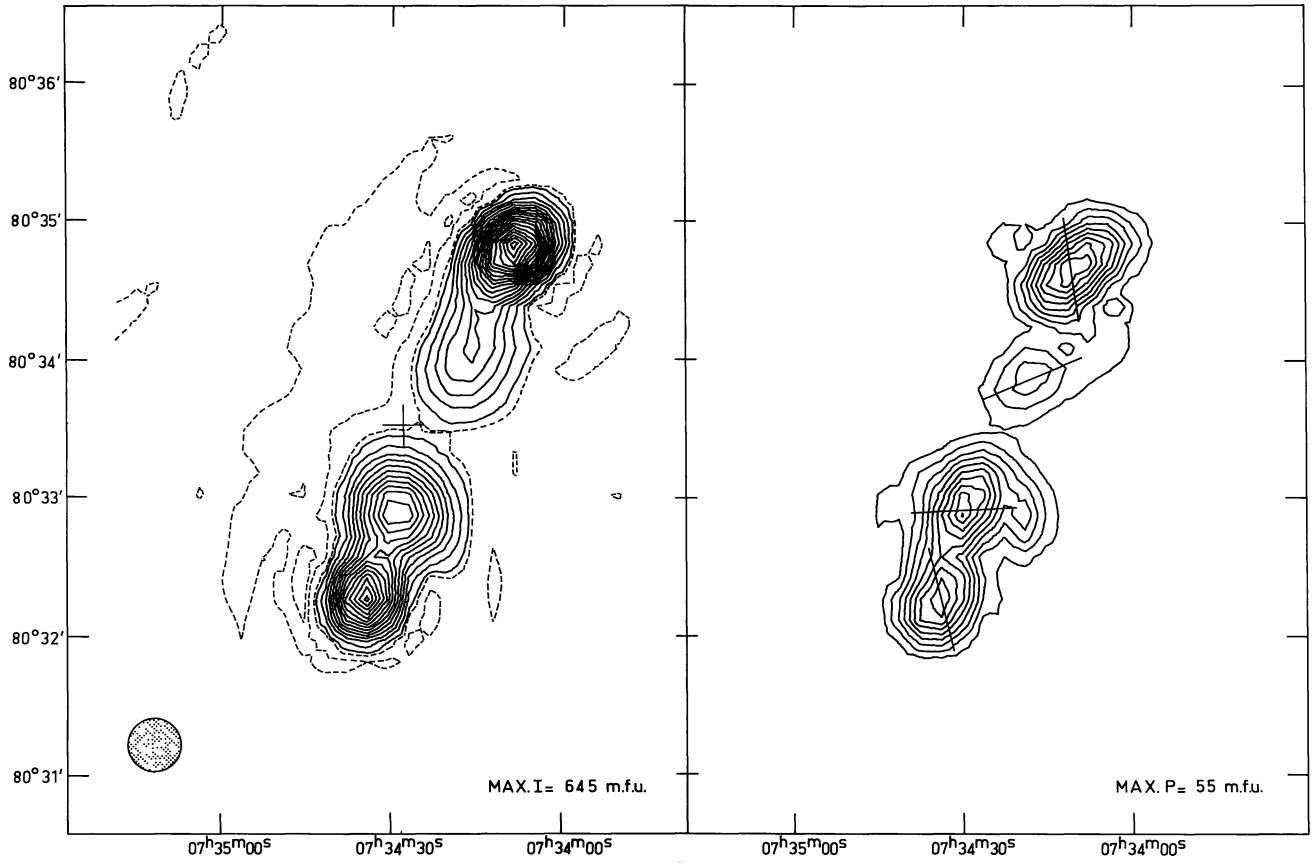


Fig. 3

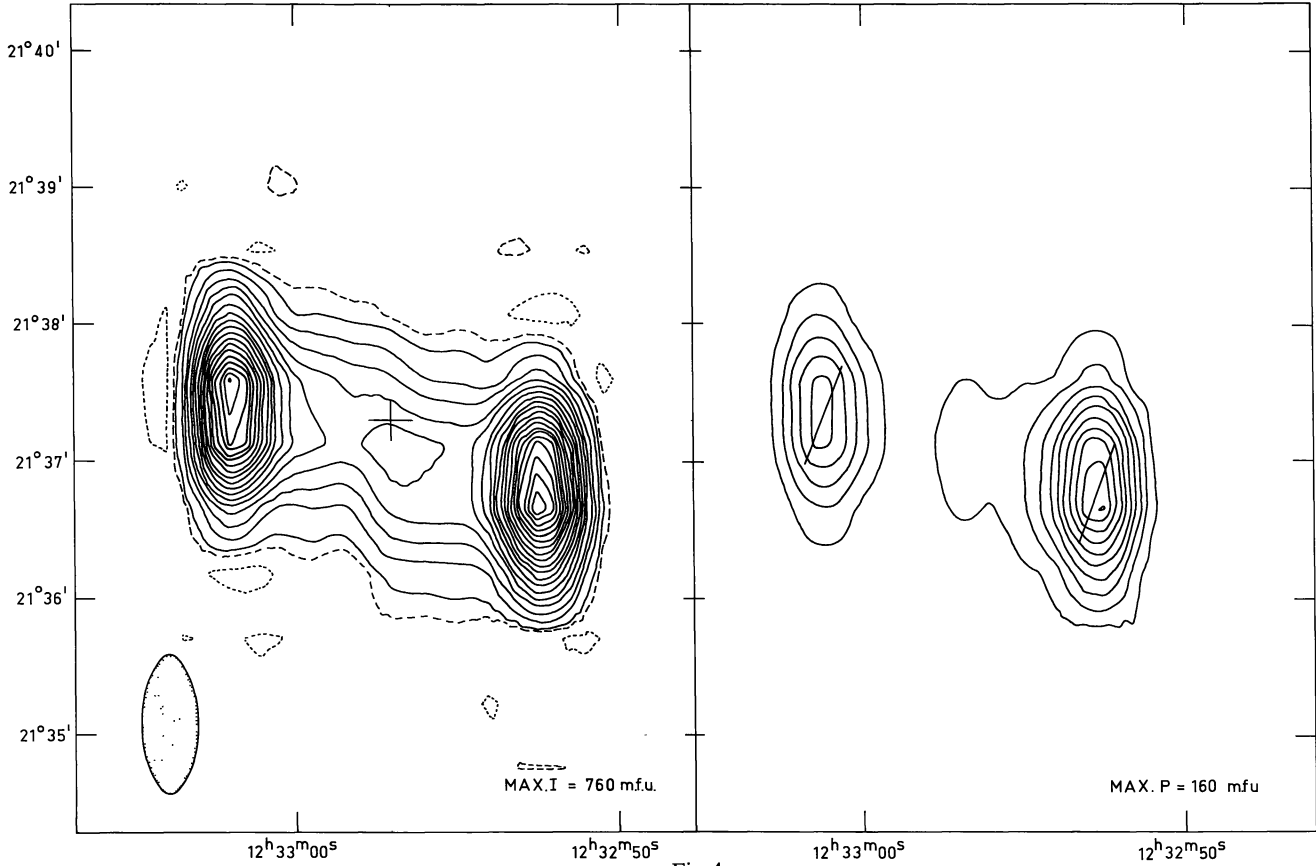


Fig. 4

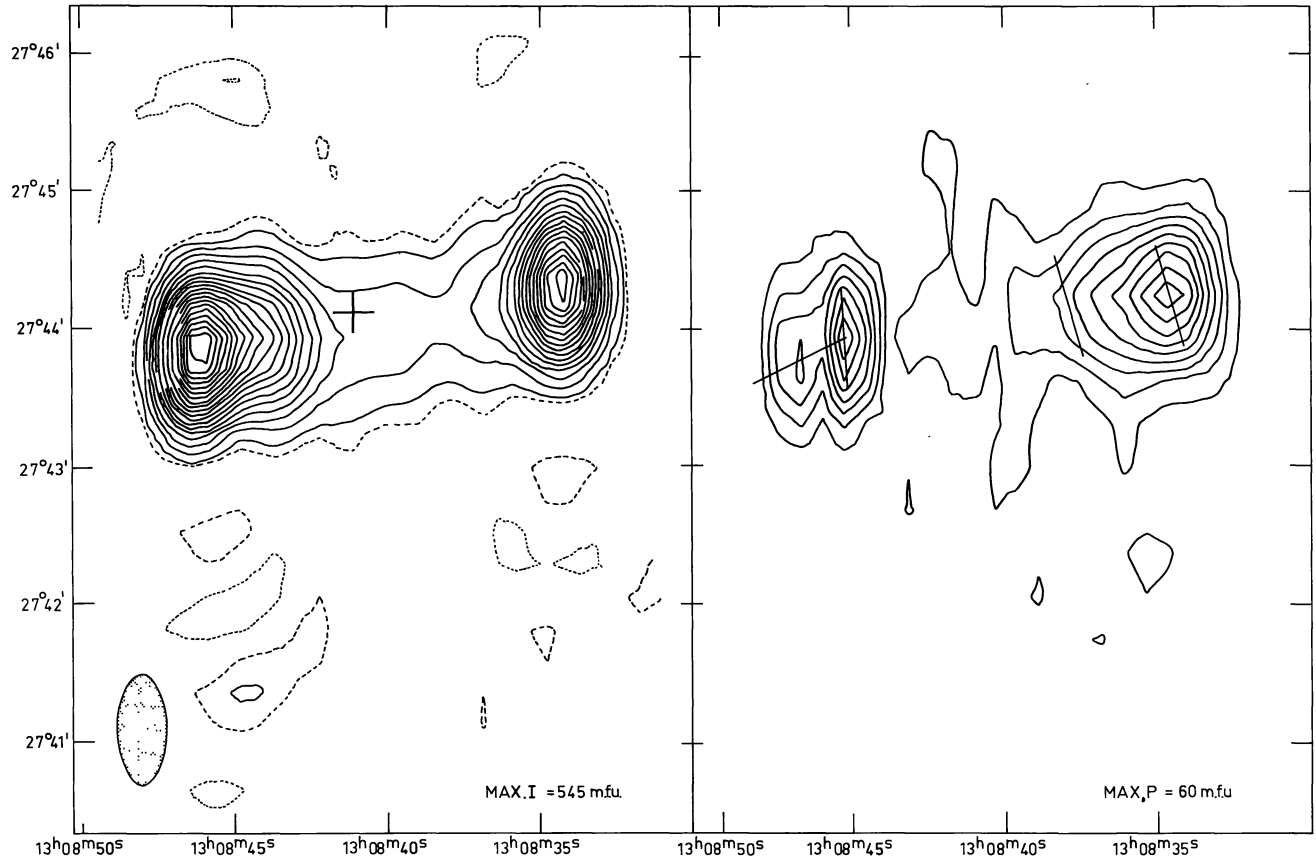


Fig. 5

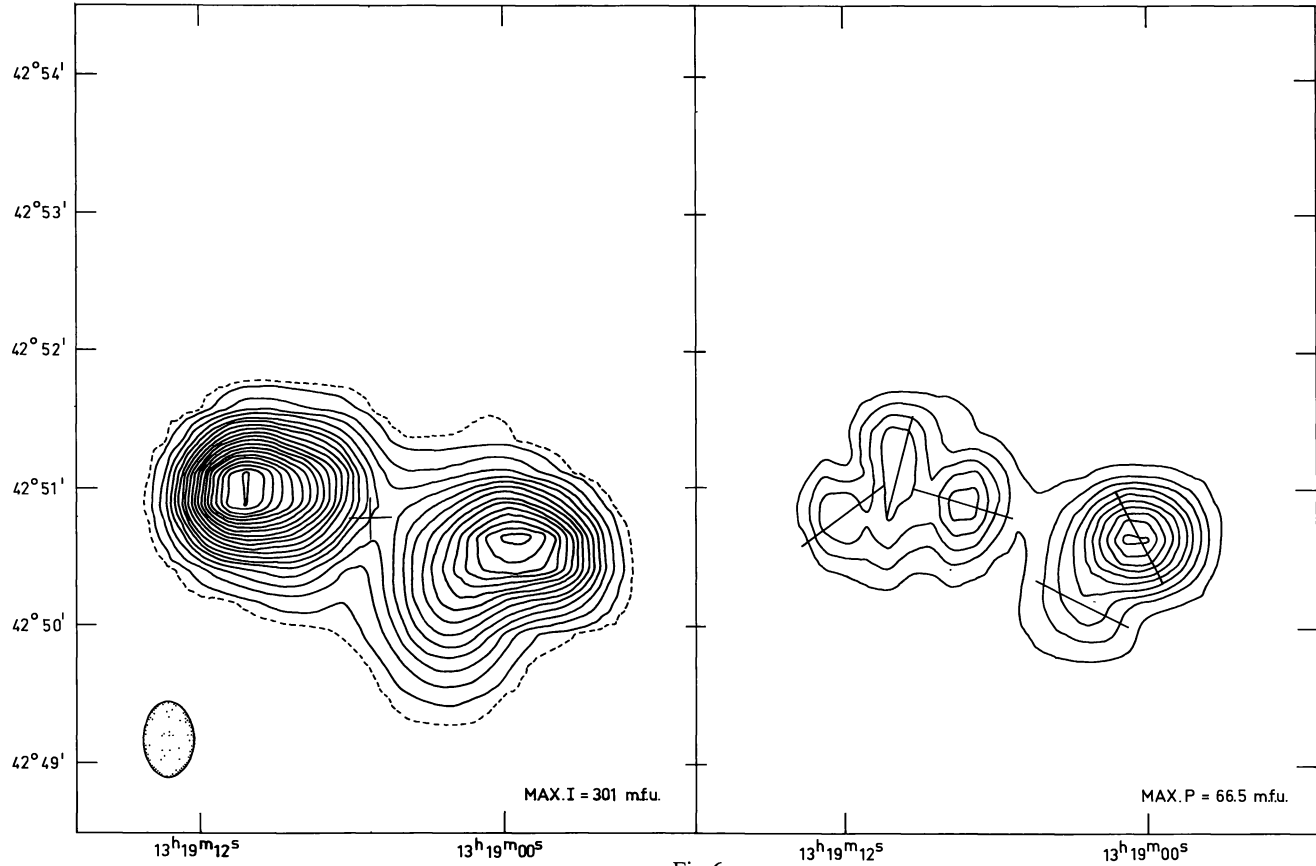


Fig. 6

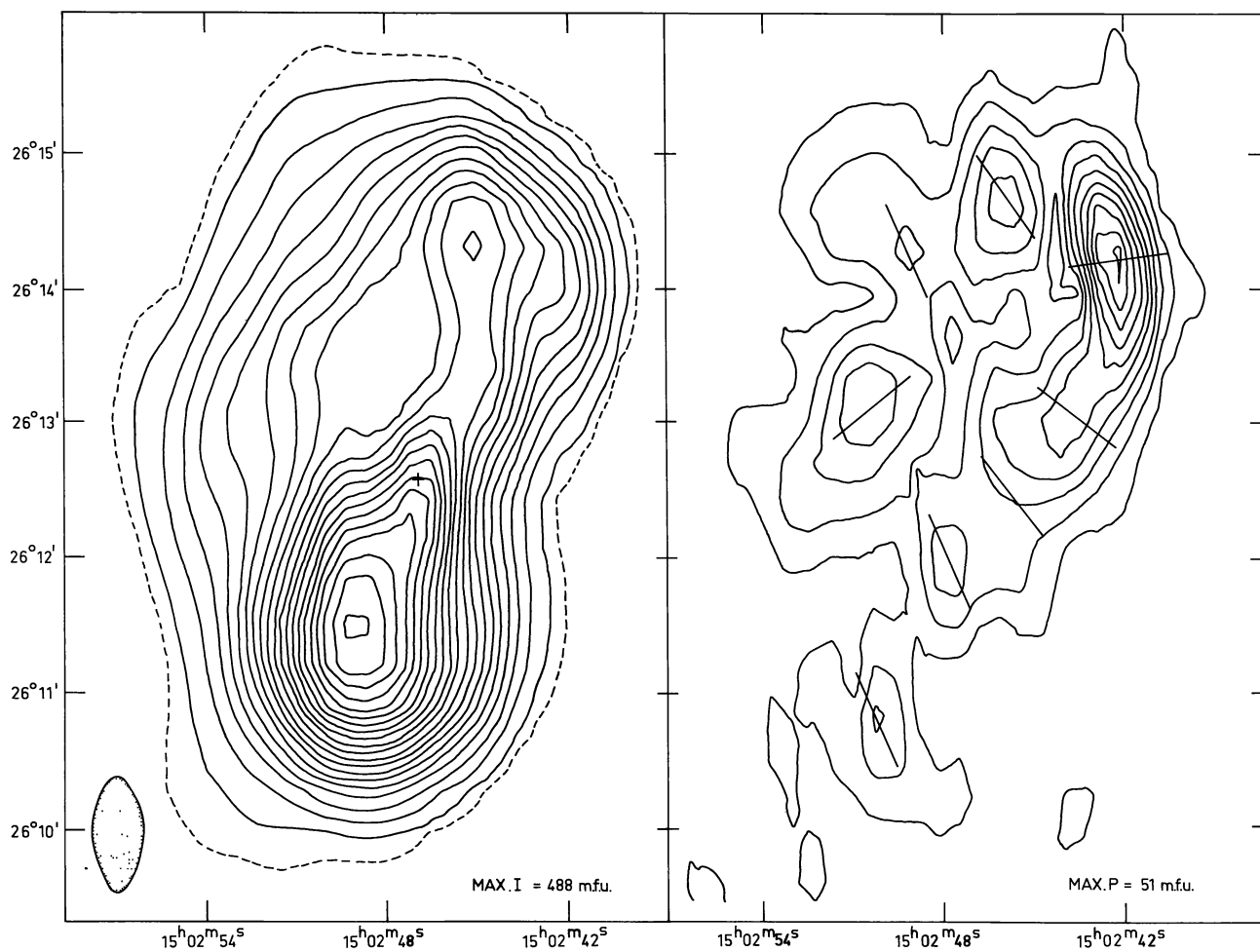


Fig. 7

Fig. 5. 3 C 284. This source is very similar to 3 C 274.1. The outer edges of the two components are again unresolved, but the inner gradients are extended further to the centre. Higher resolution observations of the east components may well show it to be double. Again the inner parts of the source are more highly polarized

Fig. 6. 3 C 285. This double source consists of two well-resolved components whose central extensions merge. The west component's total intensity and polarization distributions are very similar; the polarization is $\sim 30\%$. The east component has three polarization peaks surrounding its centre. The radial direction of the polarization vectors is suggestive of a tangential magnetic field, but this may be fortuitous and requires confirmation at a shorter wavelength (cf. Fomalont, 1972)

Fig. 7. 3 C 310. This is a large and well-resolved double source with a striking polarization structure. The stronger southern component is only weakly polarized, mostly on its SE periphery. The whole northern half of the source is characterized by a ring of polarization peaks and a polarization minimum at the total intensity maximum. Here also it is necessary to determine the rotation measure, but the P -vectors are again consistently radial to first approximation. The NW polarization peak is $\sim 30\%$. 5 GHz Westerbork results show a point component with a flux density of 0.09 ± 0.01 f.u. at a 1950 position of R.A. $15^{\text{h}}02^{\text{m}}46^{\text{s}}85 \pm 0^{\text{s}}05$, Dec. $+26^{\circ}12'35''.3 \pm 1''.0$ coincident with galaxy No. 1 of Griffin (1963). This component has a very flat spectrum ($\alpha_{1.4}^{\nu} = 0.0 \pm 0.2$)

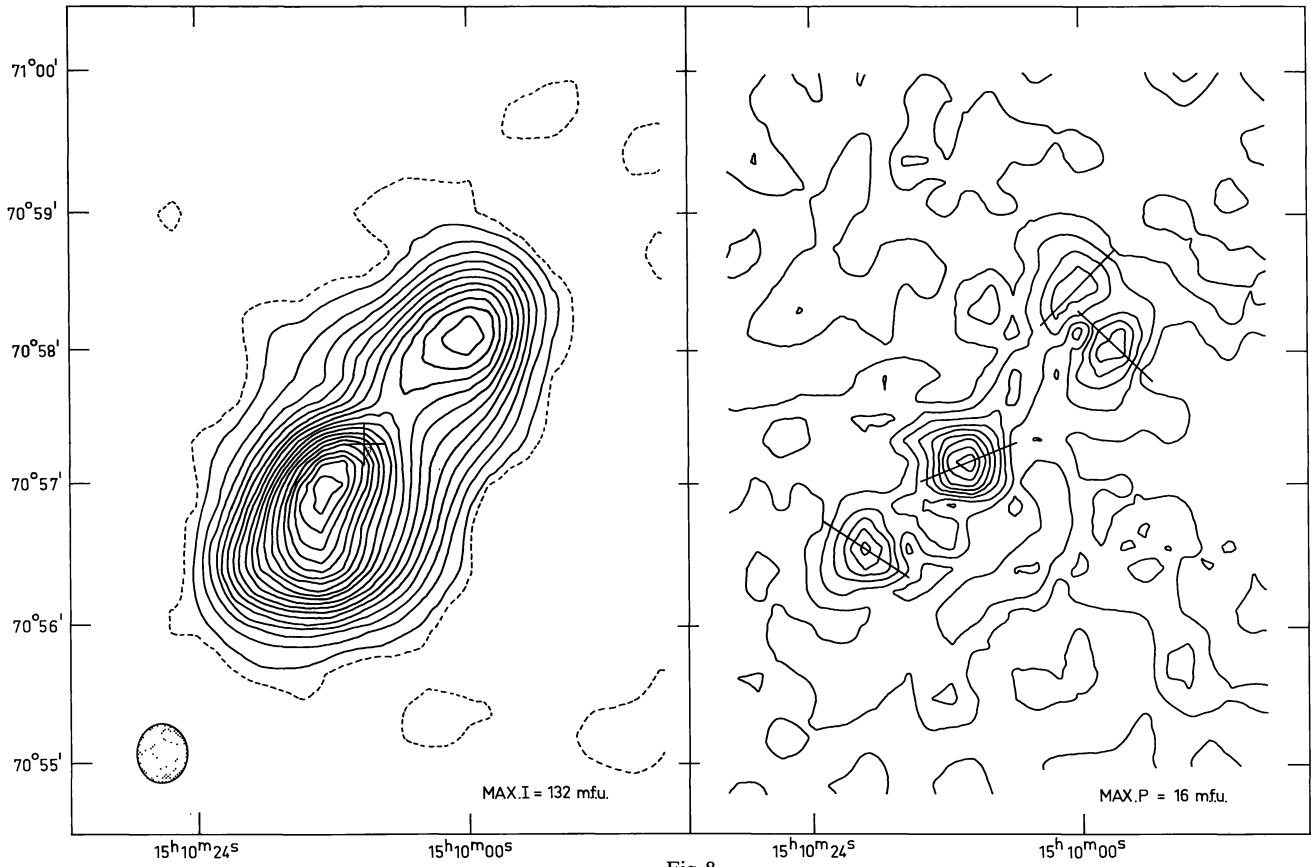


Fig. 8

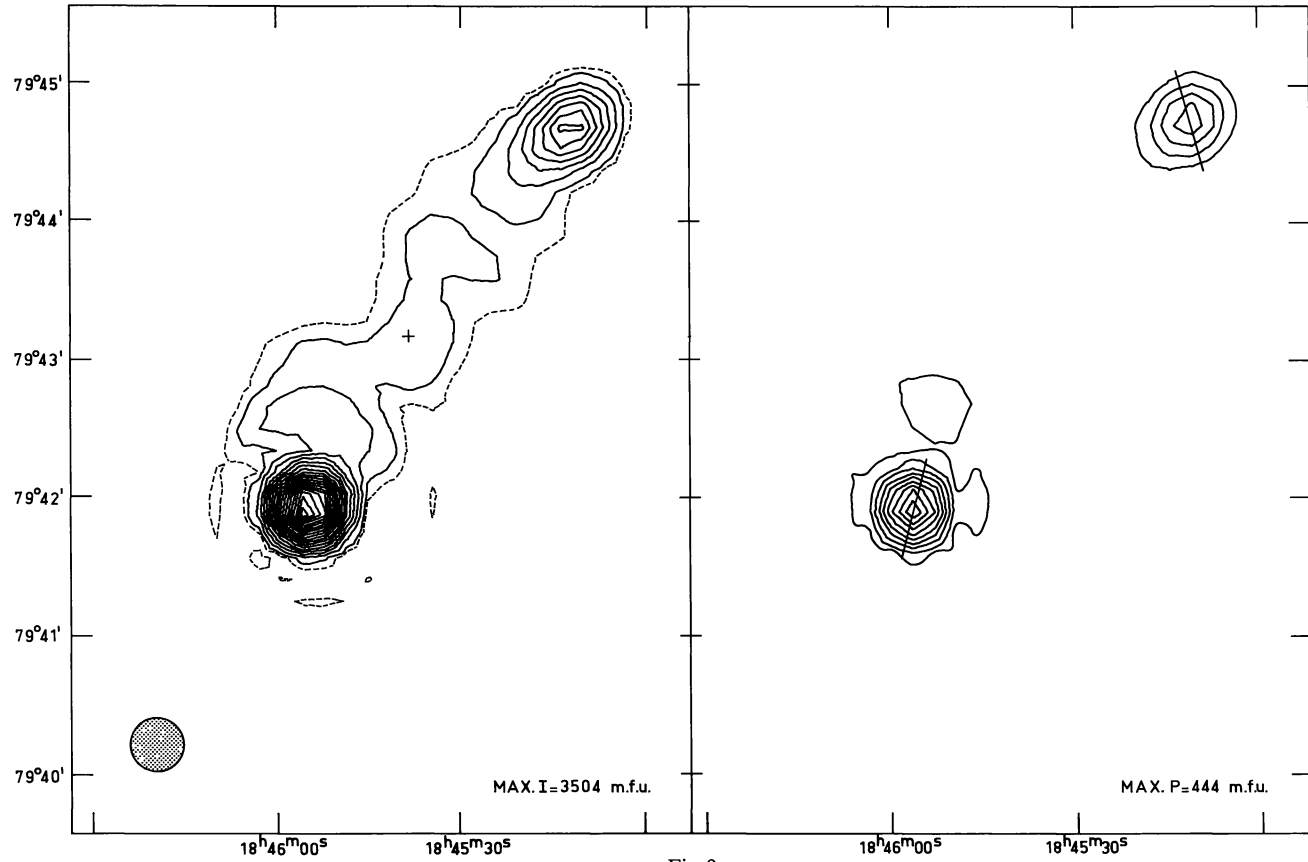


Fig. 9

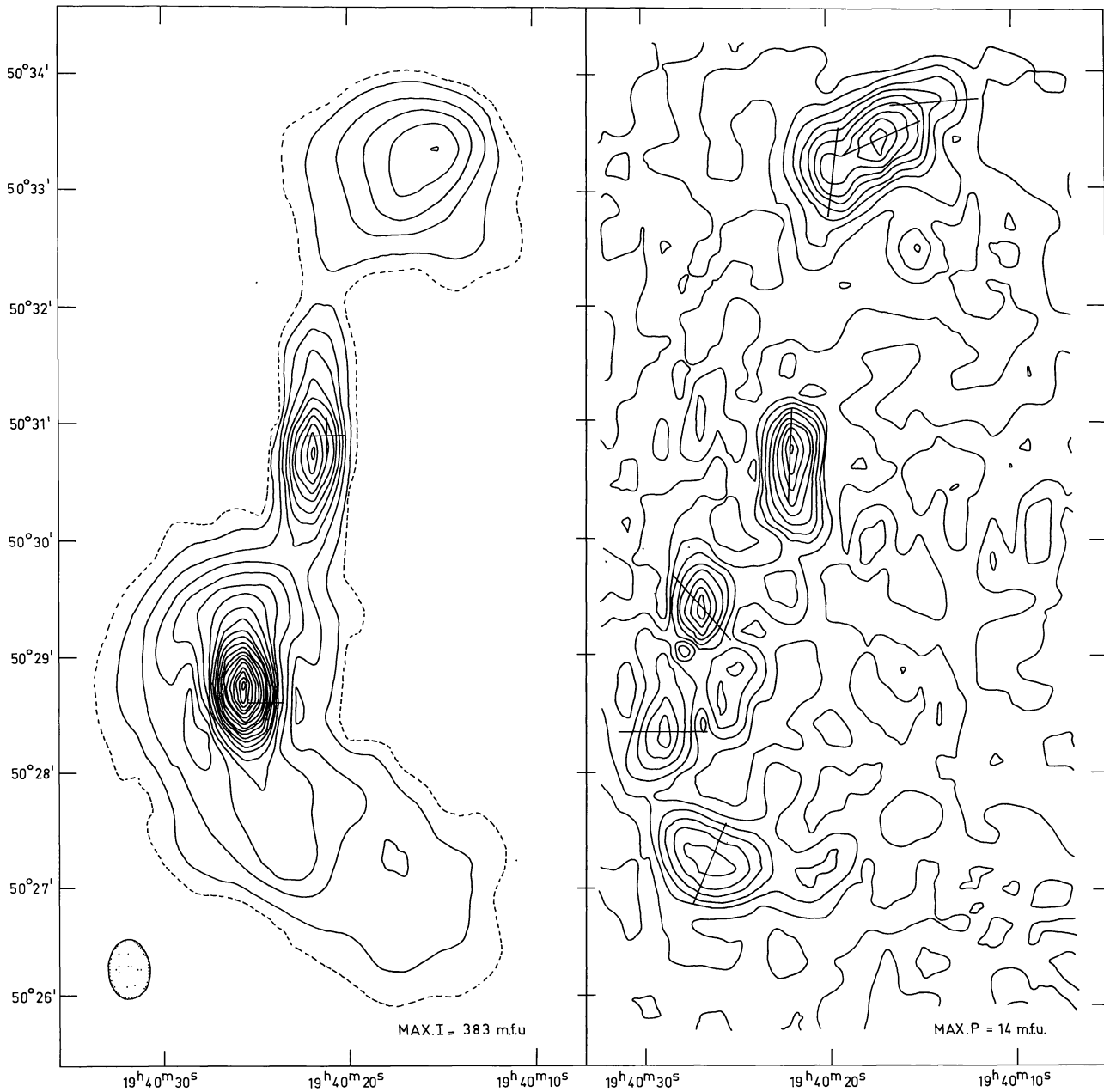


Fig. 10

Fig. 8. 3 C 314.1. This is also a relaxed double source with merging components. Here all of the six or more relative maxima in P lie on the gradients of the total intensity components, similar to the east component of 3 C 285 and the northern half of 3 C 310. The total intensity peaks are coincident with relative minima in polarization intensity. This is the only source in our sample where we are seriously noise limited

Fig. 9. 3 C 390.3. A simple double source, discussed by Harris (1972), with a weak bridge. 2.7 and 5 GHz results of Harris show a 0.35 f.u. point source coincident with the galaxy. After subtraction of the two outer components, we obtain a 1.4 GHz flux density of 0.35 ± 0.05 f.u. for this component. The strong SE component is unresolved while the weaker NW component, unresolved perpendicular to the source axis is elongated along that axis. The NW component is polarized by $15.6 \pm 1.5\%$ in P.A. $16^\circ \pm 3^\circ$ and the SE one by $12.7 \pm 1.0\%$ in P.A. $165^\circ \pm 2^\circ$. A comparison with the results of Harris (1972) gives rotation measures of -14 ± 7 and < 4 rad. m^{-2} respectively

Fig. 10. 3 C 402. This source has two bright components, each of which is coincident with a galaxy (Macdonald *et al.*, 1968). The south component has an unresolved, weakly polarized core, superposed on the large resolved feature. The latter has a ring of polarization peaks, reaching 19% fractional polarization, whose vectors point roughly towards a common centre. The northern component, well resolved and simply structured, has a displaced $\sim 16\%$ polarization peak. At first sight the proximity of the two radio galaxies appears remarkable. However, from the radio properties of elliptical galaxies with the same optical magnitude one can deduce that the probability of such a chance coincidence is not negligible (Ekers, private communication). Apart from the two unresolved components it is impossible to tell which of the two galaxies is identified with the individual radio features

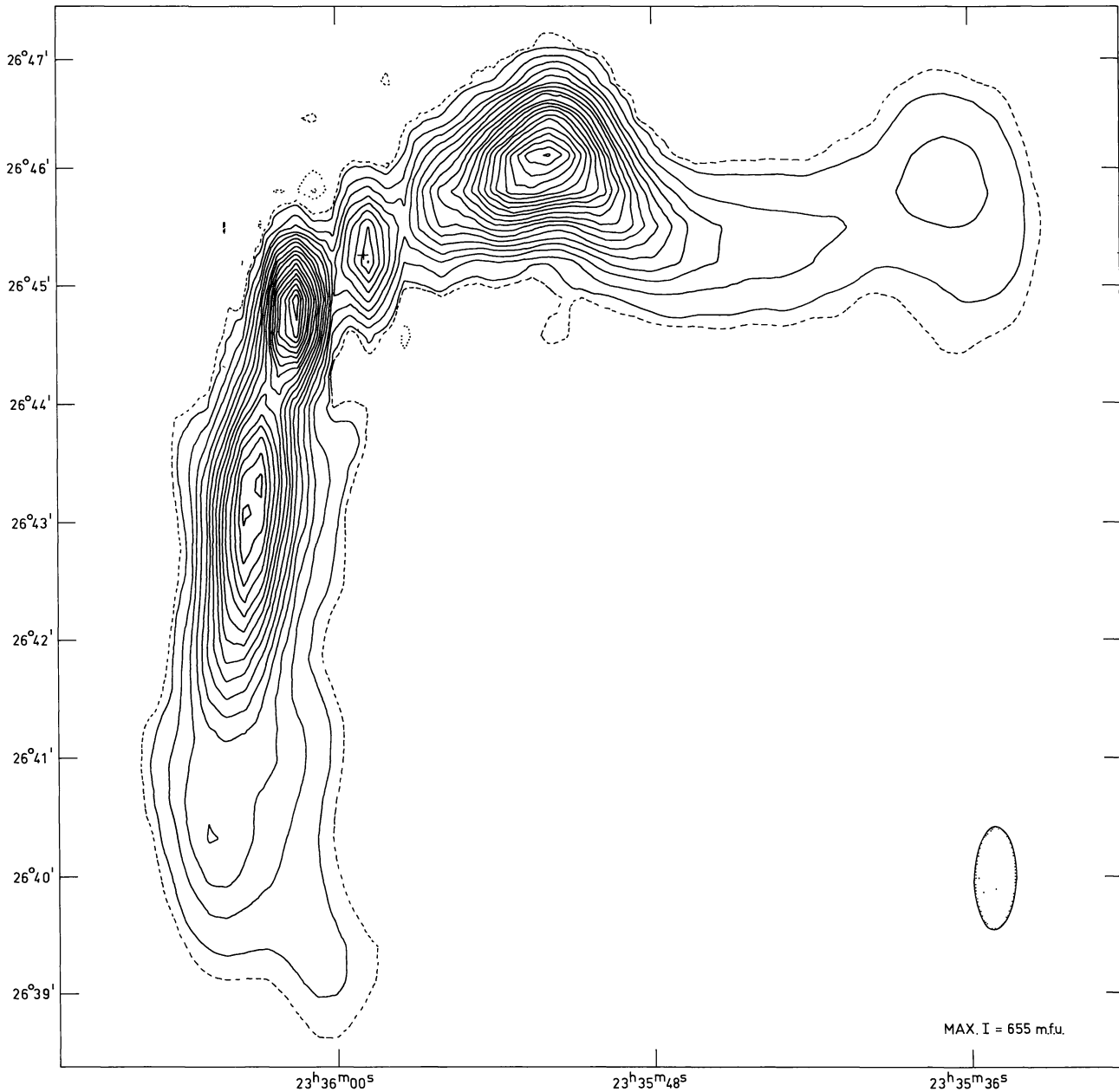


Fig. 11a

Fig. 11. 3C 465. A complex source identified with the double galaxy NGC 7720 in Abell Cluster A-2634 (Griffin, 1963). Although the whole source has a spectral index ~ -0.85 , unpublished Westerbork 5 GHz results show an unresolved component with an extremely flat spectrum coincident with the galaxy (1950 position: R.A. $23^{\text{h}}35^{\text{m}}58^{\text{s}}.92 \pm 0.05$, Dec. $+26^{\circ}45'16''.8 \pm 1''.0$, $S_{5\text{ GHz}} = 0.28 \pm 0.02$ f.u., $\alpha_{1.4\text{ GHz}}^{5.0} = 0.04 \pm 0.2$). Two radio arms stretch almost at right angles from the galaxy and trail gradually into the noise. Along the west arm abrupt changes in the polarization position angles occur; the peaks in fractional polarization are displaced from the peaks in total intensity and reach more than 25%. The south arm is much less strongly polarized

in Q and U one can obtain rough estimates for the errors in P and ϕ , namely: $\Delta P \sim 2 \text{ m.f.u.} + 5\% P$
 $+ 5\% I$

$$\Delta\phi \sim \left(\frac{1}{2} \frac{\Delta P}{P} \text{ radians} + \Delta\phi_{\text{ionosphere}} \right).$$

Here $\Delta\phi_{\text{ionosphere}}$ is the rotation in the position angles due to Faraday rotation in the ionosphere – typically $+2^\circ$ but $+5^\circ$ under extreme conditions. Of course

these error estimates cannot include effects such as a reduction of P due to a change in the position angles on a scale comparable to or less than that of the synthesized beam.

Additional verification of our estimates of instrumental errors is provided by P -maps of the unpolarized source 3C 84. The maximum polarization did not exceed 0.3% of the maximum total intensity. Thus instrumental errors in P are swamped by the 10% contour intervals.

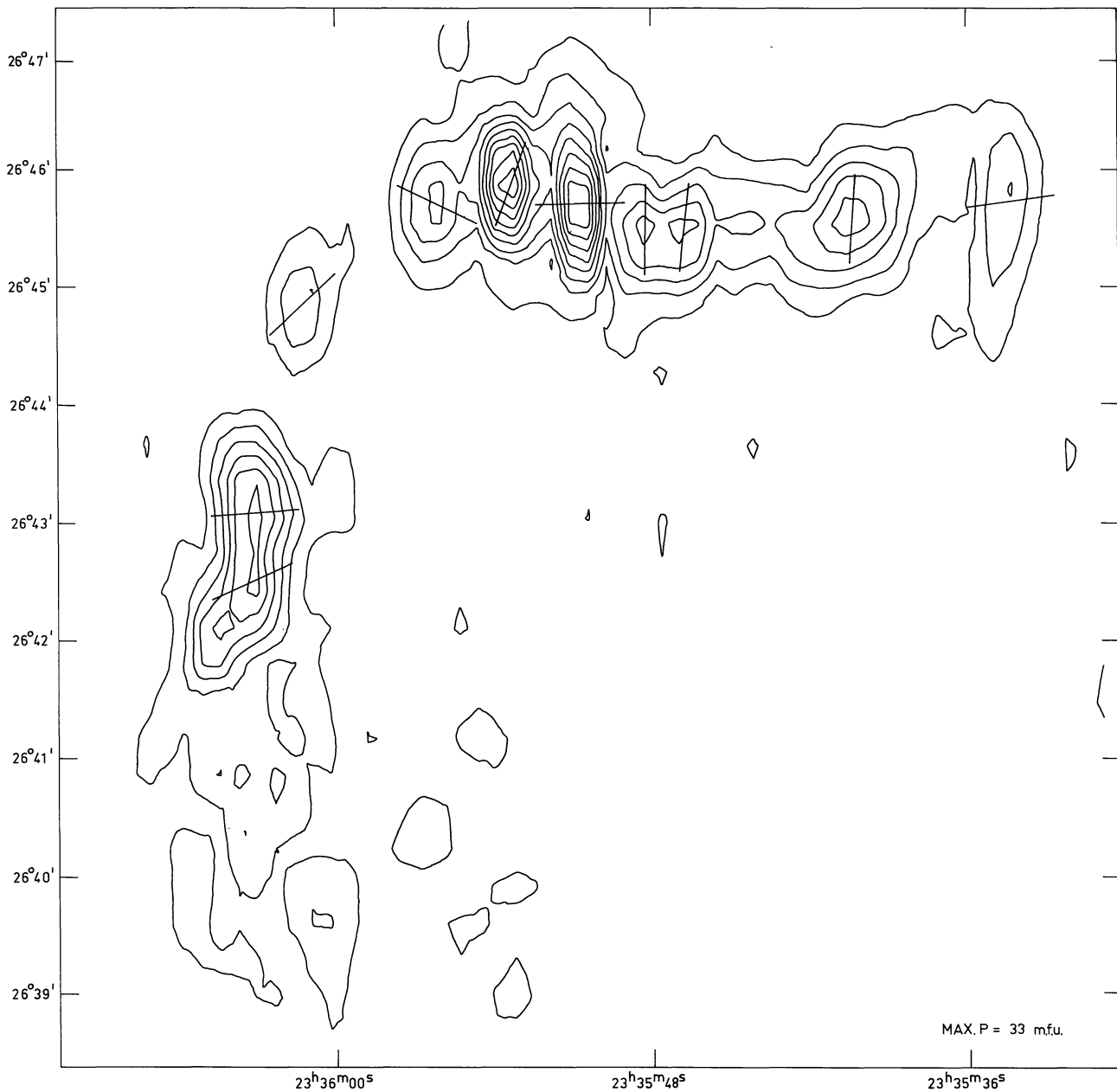


Fig. 11b

Also, from two separate observations made on both 3 C 184.1 and 3 C 465 it is clear that the polarization maps show a very high degree of repeatability.

One must exercise caution in calculating the percentage polarization from the ratios of P and I , particularly at points of the map where the gradients are steep. Slight position errors in the Stokes parameter could result in large errors in the percentages.

4. Discussion

General features of the polarization maps: – First, as one might expect, the polarization distributions are more complex than the total intensity structures.

Observations at other frequencies on sources such as 3 C 310 should reveal whether this complexity is due to geometric features of the magnetic fields within the sources or caused by differential Faraday rotation due to a thermal plasma. Values of parameters derived from the wavelength dependence of the integrated polarization properties must therefore be treated very cautiously. Secondly, for the resolved components the peaks in P do not in general coincide with the peaks in I . This indicates that in the more relaxed low brightness regions the magnetic fields have a larger scale or else the depolarization is less.

The double sources: – As we have already mentioned the structure of the sources in our sample are re-

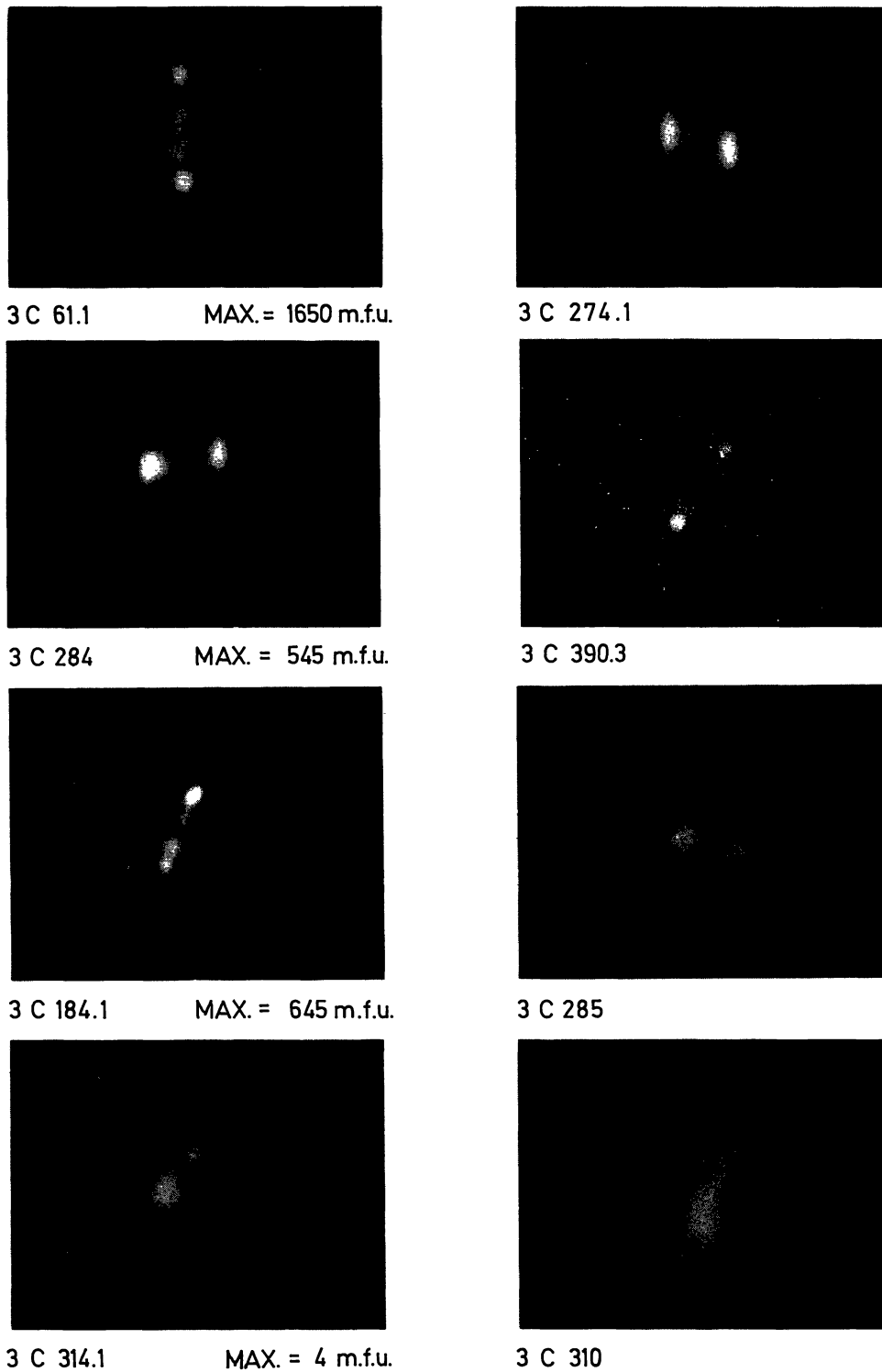


Fig. 12. Radio photographs of the simple "double" sources observed in our sample. From top to bottom the pairs are 3 C 61.1 and 3 C 274.1, 3 C 284 and 3 C 390.3, 3 C 184.1 and 3 C 285, 3 C 314.1 and 3 C 310. The brightest spot on each photograph is normalized to the maximum radio intensity MAX.I

representative of the wide range of diverse forms exhibited by strong extragalactic radio sources. Eight of them are double sources (i.e. sources containing two strong components located symmetrically with respect to the optical galaxy). We have arranged these simple double sources into a morphological sequence and

this is illustrated in Fig. 12 using radio photographs of their total intensity. The radio-photographic technique developed by Jaffe is superior to contour mapping where it is required to represent qualitatively the features of maps with large dynamic range. Our sequence runs roughly according to the relative im-

portance of the high brightness outer edges, from 3 C 390.3, 3 C 61.1 and 3 C 184.1 through 3 C 274.1, 3 C 284 and 3 C 285 to the more relaxed system of 3 C 314.1 and 3 C 310. Within the context of the ram pressure confinement model our sequence exhibits some evolutionary features. One may interpret 3 C 390.3 and 3 C 184.1 as relatively young sources in which ram pressure confinement by an intergalactic medium preserves the high brightness of the outer edges. When the expanding plasmoids are retarded sufficiently for the confinement forces to be unimportant, the components begin to expand adiabatically and evolve through a 3 C 285 stage until they resemble 3 C 314.1 and 3 C 310. The latter two sources are smooth relaxed systems with steep spectra and presumably represent the late stages of the radio phase. 3 C 61.1, 3 C 274.1 and 3 C 284, although morphologically similar to 3 C 390.3 and 3 C 184.1 are physically larger, intrinsically more powerful and considerably more distant sources. Where the outer components are unresolved and have unresolved leading edges, the polarization peaks are generally displaced inwards. In several cases the magnetic field direction seems parallel to the source axis (3 C 274.1; cf. Harris, 1972), but it is not yet clear whether this is always the case. In the well-resolved components the polarization vectors assume a radial pattern in several instances (cf. 3 C 285, 3 C 310, 3 C 402; Fomalont, 1972). This indicates circumferential magnetic fields in the more relaxed, presumably older systems. The process by which such a magnetic configuration is reached is not clear. If the components evolve into shells, tangential fields would be expected, but we have as yet no evidence for shell structure in these sources.

All of the double sources in our sample have bridges of radio emission associated with them. For 3 C 274.1, 3 C 284 and 3 C 390.3 these bridges are relatively smooth in appearance whereas those of 3 C 61.1 and 3 C 184.1 show more discreteness. One of the questions most basic to the nature of radio emission phases in the life of stellar systems concerns the interpretation of the bridges. One possibility is that the double radio source is produced by a single event in the galaxy and that the bridges are *trails* left behind as the two plasmoids ram into the intergalactic medium. Alternatively they may represent channels by which new relativistic particles are being continuously fed from the galaxy to the bright radio components. It is interesting that several of the sources studied at 5 GHz have a flat spectrum component coincident with the optical galaxies, indicating that even for old sources such as 3 C 310 the associated galaxy is still active. These “galaxy” components could well be continuously replenishing relativistic electrons in the source.

The complex sources. – We next remark on the complex structures exhibited by 3 C 465, 3 C 402 and 3 C 66 (Fig. 13). As can be seen from Table 1 these sources are

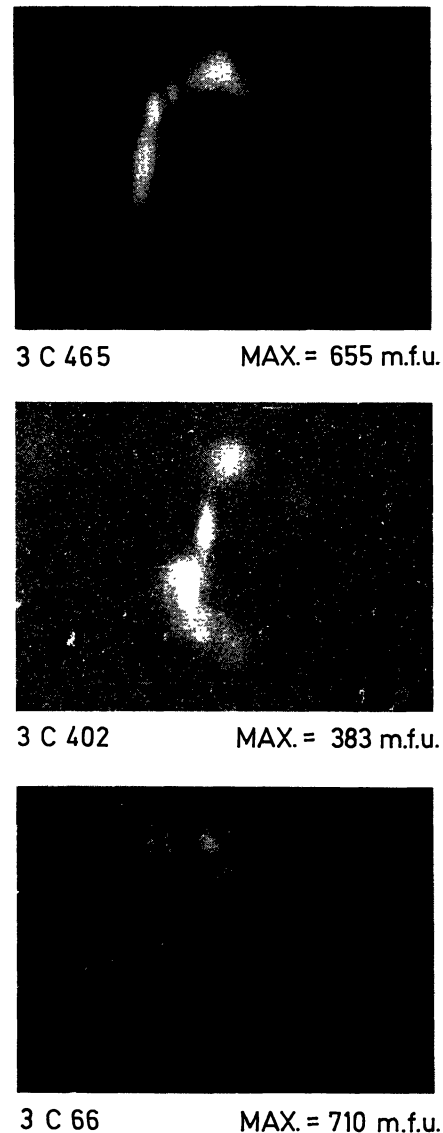


Fig. 13. Radio photographs of the complex sources observed in our sample. From top to bottom 3 C 465, 3 C 402 and 3 C 66

all intrinsically weaker than the simpler sources discussed above; their luminosities are comparable to the “head-tail” sources such as 3 C 129 or NGC 1265 known to occur in clusters of galaxies; 3 C 465 and 3 C 66 are also located in clusters. Miley *et al.* (1972) have suggested that the radio tails are caused by motion of the galaxies through an intergalactic medium during their radio emitting phases. They also interpreted 3 C 465 within this “ploughing galaxy” model as an intermediate case in which the motion of the galaxy is relatively less important. 3 C 402 is probably a superposition of two emitting galaxies (see Fig. 10). However, it is easy to imagine its apparent structure as a different projection of 3 C 465. The structure of 3 C 66 does not suggest so simple a relation to that of 3 C 465, although their chief difference is conceivably one of projection also.

Here we have attempted to show qualitatively how our 1.4 GHz data can be interpreted within an evolutionary scheme of extragalactic radio sources. As we have stated in the introduction more quantitative remarks must await observations at several wavelengths. Such measurements are now being made and promise to place useful limits on mechanisms for radiation and confinement within the sources.

References

- Baars, J. W. M., Hooghoudt, B. 1973, *Astron. & Astrophys.* (in press)
 Berkhuijsen, E. M., van de Hulst, H. C., Spoelstra, T. A. 1973 (in preparation)
 Burbidge, E. M., Strittmatter, P. A. 1972, *Astrophys. J.* **172**, L 37
 Casse, J. L., Muller, C. A. 1973, *Astron. & Astrophys.* (in press)
 Fomalont, E. B., Högbom, J. 1973 (in preparation)
 Gardner, F. F., Whiteoak, J. B. 1971, *Australian J. Phys.* **24**, 899
 Griffin, R. F. 1963, *Astron. J.* **68**, 421
 Harris, A. 1972, *Monthly Notices Roy. Astron. Soc.* **158**, 1
 Kellermann, K. I., Pauliny-Toth, I. I. K., Williams, P. J. S. 1969, *Astrophys. J.* **157**, 1
 Kronberg, P. P. I., Strom, R. G. 1973 (in preparation)
 Macdonald, G. H., Kenderdine, S., Neville, A. C. 1968, *Monthly Notices Roy. Astron. Soc.* **138**, 259
 Mackay, C. D. 1969, *Monthly Notices Roy. Astron. Soc.* **145**, 31
 Miley, G. K., Perola, G. C., van der Kruit, P. C., van der Laan, H. 1972, *Nature* **237**, 269
 Miley, G. K. 1973, *Astron. & Astrophys.* **26**, 413
 Mitton, S. 1972, *Monthly Notices Roy. Astron. Soc.* **155**, 373
 Weiler, K. W. 1973, *Astron. & Astrophys.* **26**, 403
 Westerhout, G., Seeger, C., Brouw, W. N., Tinbergen, J. 1962, *Bull. Astron. Inst. Neth.* **16**, 187

G. K. Miley
 H. van der Laan
 Sterrewacht Leiden
 Leiden-2401, The Netherlands